



**HAL**  
open science

# Effects of particle mixtures and nozzle geometry on entrainment into volcanic jets

D.E. Jessop, A. M. Jellinek

► **To cite this version:**

D.E. Jessop, A. M. Jellinek. Effects of particle mixtures and nozzle geometry on entrainment into volcanic jets. *Geophysical Research Letters*, 2014, 41 (11), pp.3858-3863. 10.1002/2014GL060059 . hal-01637505

**HAL Id: hal-01637505**

**<https://uca.hal.science/hal-01637505>**

Submitted on 17 Nov 2017

**HAL** is a multi-disciplinary open access archive for the deposit and dissemination of scientific research documents, whether they are published or not. The documents may come from teaching and research institutions in France or abroad, or from public or private research centers.

L'archive ouverte pluridisciplinaire **HAL**, est destinée au dépôt et à la diffusion de documents scientifiques de niveau recherche, publiés ou non, émanant des établissements d'enseignement et de recherche français ou étrangers, des laboratoires publics ou privés.

RESEARCH LETTER

10.1002/2014GL060059

Key Points:

- Source geometry plays an important role in entrainment
- Certain sizes of particles combine with source effects to modify entrainment
- Cloud structure and deposits change during an eruption for same conditions

Supporting Information:

- Readme
- Table S1
- Table S2
- Figure S1
- Figure S2

Correspondence to:

D. E. Jessop,  
djessop@eos.ubc.ca

Citation:

Jessop, D. E., and A. M. Jellinek (2014), Effects of particle mixtures and nozzle geometry on entrainment into volcanic jets, *Geophys. Res. Lett.*, 41, doi:10.1002/2014GL060059.

Received 28 MAR 2014

Accepted 23 MAY 2014

Accepted article online 27 MAY 2014

## Effects of particle mixtures and nozzle geometry on entrainment into volcanic jets

D. E. Jessop<sup>1</sup> and A. M. Jellinek<sup>1</sup>

<sup>1</sup>Department of Earth, Ocean and Atmospheric Sciences, University of British Columbia, Vancouver, British Columbia, Canada

**Abstract** Efficient turbulent entrainment causes otherwise dense volcanic jets to rise high into the atmosphere as buoyant plumes. Classical models suggest that the inflow of air is 10–15% of the axial velocity, giving predictions for the height of the plume and, in turn, the composition and structure of the resulting umbrella clouds. Crucially, entrainment is assumed independent of source geometry and mechanically unaffected by the pyroclastic mixture properties. We show that particle inertia and vent geometry act to modify the shape of the largest eddies defining the jet's edge and thus entrainment of the ambient. Whereas particle-free flows are essentially unaffected by vent shape, entrainment into particle-laden flows is enhanced for flared vents and reduced for cylindrical vents. Our results predict that vent erosion during an explosive eruption reduces the height of volcanic jets, alters the structure and sedimentation regime of the umbrella cloud, and the resulting deposit.

### 1. Introduction

The rise and spread of initially dense volcanic jets into the atmosphere is governed by the entrainment and heating of ambient air as well as the source conditions and environmental stratification [Morton *et al.*, 1956; Woods, 1995]. Indeed, the rise height,  $H_0$ , scales as

$$H_0 \sim (2\alpha_e)^{-1/2} f_0^{1/4} N^{3/4}, \quad (1)$$

where  $\alpha_e$  is the entrainment coefficient (see below),  $f_0$  is the buoyancy flux at the source, and  $N$  is the buoyancy frequency defined by the density stratification of the atmosphere [Morton *et al.*, 1956; Carazzo *et al.*, 2008]. Whether jets ultimately ascend as buoyant plumes to form an umbrella cloud or collapse as a fountain to produce devastating pyroclastic flows depends on whether sufficient atmosphere is incorporated to drive a buoyancy reversal [Woods, 2010]. Studies of the jet's motion relate the entrainment velocity to some fraction of the axial velocity [Morton *et al.*, 1956]. Experiments using particle-free jets show that the entrainment coefficient given by the ratio of these two velocities,  $\alpha_e \approx 10\text{--}15\%$  depending on whether the jet is momentum or buoyancy dominated [Fischer *et al.*, 1979; Linden, 2002]. Recent studies highlight that  $\alpha_e$  depends on the buoyancy of the jet and can vary by as much as a factor of 2 along the height of a jet as the buoyancy and velocity profiles evolve with distance [Papanicolaou and List, 1988; Wang and Law, 2002; Kaminski *et al.*, 2005; Carazzo *et al.*, 2006]. However, in the current state-of-the-art, the entrainment coefficient has no dependence on the vent size, geometry, or mass loading in particles. Mechanical erosion during an eruption can, for example, cause vent geometry to change from a cylindrical to an outwardly flared geometry. Such a geometric change affects the trajectories of entrained inertial particles and can guide the initial momentum flux of the mixture. Although the effect of vent size has been discussed in the context of the supersonic to subsonic transition in overpressured systems [Wilson *et al.*, 1980; Woods and Bower, 1995], the explicit mechanical effect of vent geometry on entrainment rates is an effect that has previously been ignored.

Although explosive volcanic eruptions are rich in particles of a wide range of sizes (e.g., pumice and ash), few studies address the influence of particles on the mechanics of entrainment and mixing. In particular, whereas entrained particles impart additional inertial and buoyancy effects, most previous studies of particle-laden jets [e.g., Carey *et al.*, 1988; Veitch and Woods, 2002] assume that particles contribute only to the state of the jet. Whether and how these particles influence the entraining properties of the largest eddies depends on the extent to which they are coupled to the flow [Crowe *et al.*, 1997]. The inertial response time of entrained particles is characterised by  $\tau_p = \rho_p d_p^2 / (18f\mu)$ , where  $\rho_p$  and  $d_p$  are the particle

density and diameter, respectively,  $\mu$  is the fluid viscosity, and  $f$  is a drag factor of  $\mathcal{O}(1)$  for the flows studied here [Burgisser et al., 2005; Carazzo and Jellinek, 2012], and the time scale for the overturn of eddies defining the edge of a volcanic jet is given by  $\tau_f = l_e/u_e$  ( $l_e$  and  $u_e$  are length and velocity scales for the eddy, respectively). For example, where  $\tau_p$  is comparable to  $\tau_f$ , these particles will be sequestered to the margins of these motions and influence their angular momentum and the exchange of momentum with the ambient atmosphere as well as internally [Elghobashi, 1994; Crowe et al., 1997; Raju and Meiburg, 1997; Burgisser et al., 2005; Dufek and Bergantz, 2007]. The ratio of these time scales is the Stokes number,  $St = \tau_p/\tau_f$ , and these so-called “Stokes number effects” enter, where  $St \sim 0.1-1$  [Raju and Meiburg, 1997; Crowe et al., 1997]. In general, although important in the cloud, particle settling is slow in comparison to eddy overturn in the jet and so we neglect it here [Carazzo and Jellinek, 2012].

In order to entrain ambient fluid, the eddies that define the edges of a turbulent jet must penetrate, deform, and overturn stabilising density interfaces that define the environmental stratification. The extraction of kinetic energy to do the work of this mechanical mixing is conventionally expressed as a Richardson number,  $Ri = g'b/\bar{u}^2$ , where  $b$ ,  $\bar{u}$ , and  $g'$  are the local jet radius, mean axial velocity, and reduced gravity, respectively, which expresses the local balance between destabilising inertial and stabilising buoyancy forces [Linden, 1973, 1979]. Particles with large  $St$  contribute to the inertial forces in potentially complicated ways [Elghobashi, 1994]. Thus, to map a parameter space, it will be more useful to define  $Ri$  at the source,  $Ri_0 = g'_0 r_0/\bar{u}_0^2$  (in general,  $Ri \propto |Ri_0|$ ), where a subscript 0 refers to the value at the source and jet width here is equal to the nozzle radius,  $r_0$ . These parameters are based on the source conditions that we control externally. We return to this issue below.

Given that the efficiency of entrainment ultimately determines whether a given eruption will form a stable cloud or a pyroclastic flow [Woods and Caulfield, 1992], the lack of information on how particles coupled to the flow affect entrainment is an alarming knowledge gap for volcanic hazard assessment. Accordingly, we use analog experiments conducted under  $St \sim 0.1-1$  and theory to build understanding of the effect of particle inertia on the motions that ultimately govern entrainment into volcanic jets. We investigate two issues: the first is simply to characterise how particles influence the entrainment properties in jets from a quasi-point source, which is the usual setup for these problems [Woods, 2010; Carazzo and Jellinek, 2012]; second, we explore whether the results change if the analog volcanic jet is erupted from flared rather than cylindrical sources. Significantly, we will show that vent erosion combined with  $St \sim 0.1-1$  particles will increase entrainment through their profound effect on the structure of the motions governing entrainment.

## 2. Model

Under steady state conditions, conservation of volume,  $q$ , momentum,  $m$  and buoyancy,  $f$ , in a turbulent, self-similar, isothermal jet with a “top-hat” radial velocity profile is expressed by the following [cf. Morton et al., 1956; Woods, 2010]:

$$\frac{dq}{dz} = 2\alpha_e m^{1/2}, \quad m \frac{dm}{dz} = g'q^2, \quad \frac{df}{dz} = -N^2 q, \quad (2)$$

where  $q = b^2 \bar{u}$ ,  $m = b^2 \bar{u}^2$ , and  $f = g'q$  [Woods, 2010].

Entrainment causes a rising jet to increase in radius against the stabilising influence of environmental stratification, an effect which is expressed through  $Ri$ . Thus, we write  $b = q/m^{1/2}$ ,  $Ri = \beta |Ri_0|$  and differentiate with respect to height to obtain

$$\frac{db}{dz} = 2\alpha_e - \beta \frac{Ri_0}{2} = \tan \theta. \quad (3)$$

With (3) we use experimental measurements of the jet angle  $\theta$  (Figure 1) to obtain  $\alpha_e$  and  $\beta$  as functions of  $\theta$  and  $Ri_0$ . As a final remark here,  $|Ri_0| \propto 1/\bar{u}_0^2$  and thus  $1/\beta$  provides a metric for the effects of particle inertia and vent geometry on mixing.

## 3. Experiments

We use the method of Carazzo and Jellinek [2012] to inject a mixture of particles and fresh water at a fixed rate at the base of a 20 cm deep layer of salt water overlain by a 40 cm deep layer of freshwater in a 1 m  $\times$  1 m  $\times$  0.8 m tank. For simplicity, we choose a single density interface to mimic effects related to a

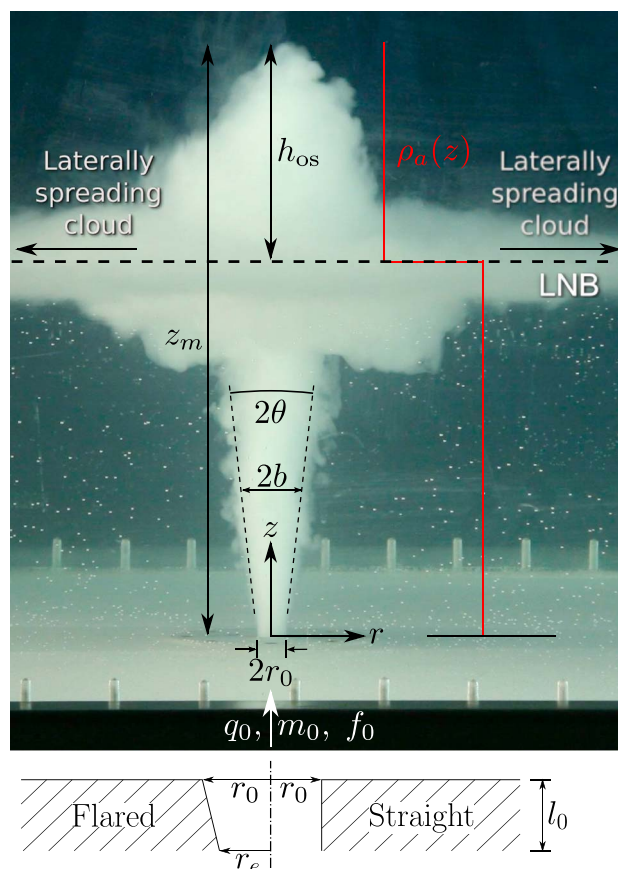


**Figure 1.** (top) Definition of parameters used in this study superimposed on an experiment image. Volume ( $q_0$ ), momentum ( $m_0$ ), and buoyancy fluxes ( $f_0$ ) are supplied at the source and enter the tank through a nozzle with exit radius  $r_0$ . The jet rises with width,  $2b$ , in a stratified environment characterised by  $\rho_a(z)$  to a maximum height,  $z_m$ , before spreading laterally as a cloud at the level of neutral buoyancy (LNB). The distance between  $z_m$  and the LNB is the overshoot height,  $h_{os}$ . The angular spread of the jet,  $2\theta$ , is measured from the outlet to the point at which the cloud forms. (bottom) A schematic of the geometry of flared and straight nozzles. The nozzles have entry and exit radii,  $r_e$  and  $r_0$ , respectively, and depth  $l_0$ . See also supporting information for details of the nozzle geometries.

more realistic quasi-linear stratification, an approximation that is appropriate provided that the buoyancy frequencies of the analog and natural cases are scaled carefully [Fan, 1967; Carazzo and Jellinek, 2012]. To map the effects of vent geometry and  $St$  on entrainment rates over a range of  $Ri_0$  appropriate for natural eruptions, we inject the particle-water mixtures with specified properties (cf. Table 1 and Figure 2) through a nozzle with an aspect ratio  $\epsilon = r_0/l_0$  and flare angle,  $\theta_{nozzle}$  that we control (see supporting information and Figure 1 (bottom)). We cover a range of source conditions which correspond to those seen in nature, namely  $Ri_0 = 10^{-5} - 10^{-1}$  and the total particle volume fraction,  $\phi = 10^{-4} - 10^{-1}$  [cf. Carazzo and Jellinek, 2012, Figure 3]. Finally, we measure steady state entrainment for given conditions by determining the angular spread,  $\theta$  as defined in Figure 1, of the jet from the vertical from a stack of images taken with a digital single-lens reflex camera recording at 1 frame per second, and fitting (3) to this data.

#### 4. Results

Figure 2 shows  $\theta$  as a function of  $Ri_0$ . We also make a qualitative comparison (insets) between our experiments and two major volcanic eruptions of recent times, Mt. St. Helens, 22 July 1980 and Grímsvötn 21–28 May 2011. We group the data according to nozzle geometry and particle concentration. We explore particle-free, dilute, and particle-rich jets erupted from cylindrical and flaring nozzles. Using a weighted least squares regression, we fit the model given by (3) to the data for each set of experiments (the fitted parameters can be found in the supporting information). Our results for broad, straight nozzles are limited by practical considerations and do not constrain the model. We show that  $\alpha_e$  decreases from 0.158 for flared

**Table 1.** Properties of Particles (Finely Ground Silica and Graded Silica Sand) Used in Our Experiments: Mean Particle Size,  $\bar{d}_p$ ; Standard Deviation of Particle Size Distribution,  $\sigma_{d_p}$ ; Particle Density,  $\rho_p$ ; Particle Relaxation Time,  $\tau_p$ ; Stokes Number,  $St^a$

	$\bar{d}_p/(\mu\text{m})$	$\sigma_{d_p}/(\mu\text{m})$	$\rho_p/(\text{g}/\text{cm}^3)$	$\tau_p/(\text{s})^b$	$St/(-)^c$
Fine silica	67.8	27.2	2.52	$1.83 \times 10^{-4}$	0.25
Silica sand	251.1	76.2	2.50	$1.19 \times 10^{-3}$	1.56

<sup>a</sup>Densities were determined by volume displacement and size distributions were determined by passing the materials through a graded range of sieves. The particles were approximately normally distributed and well sorted.

<sup>b</sup>For a viscosity of  $\mu = 10^{-3}$  Pa s (plain water at 20°C).

<sup>c</sup>Experimentally confirmed estimate for  $\tau_f \sim 10r_0/\bar{u}_0$ .

nozzles to 0.096 for narrow nozzles, and it has a value of 0.149 for particle-free flows, consistent with published data [Fischer et al., 1979; Linden, 2002]. The parameter  $\beta$  increases from 14.3 for flared nozzles to 345.4 for narrow nozzles and is 293.3 for the particle-free flows.

### 5. Discussion and Applications to Volcanic Jets

Our results show that high concentrations of  $St \sim 0.1$ –1 particles will reduce entrainment into jets erupted from cylindrical sources and enhance the inflow of ambient fluid when the source is flared. Physically, entrainment is governed ultimately by the extent to which the largest eddies defining the edge of the jet penetrate and overturn the ambient fluid. The penetration distance  $h \sim b$  must depend on both the shape

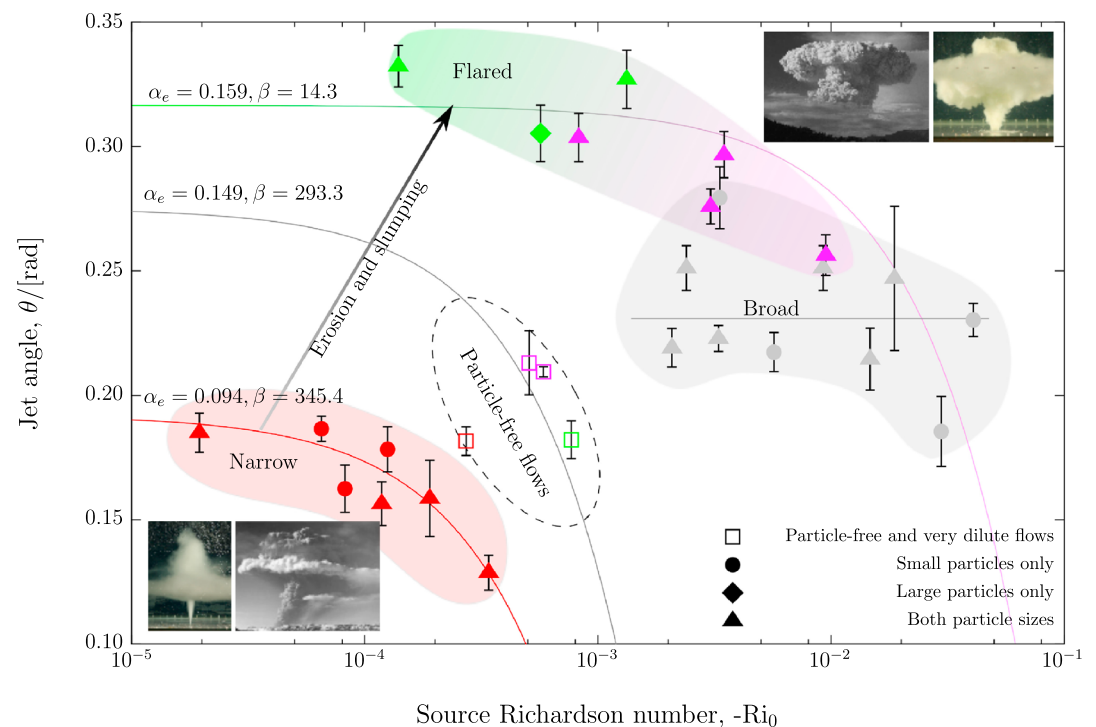


**Figure 2.** Regime diagram for the jet angle as a function of source Richardson number. Distinct behaviors are seen for narrow (red), broad (grey), and flared (green and magenta) nozzles, and also for particle-laden, particle-free, and very dilute jets. The flare angles,  $\theta_{nozzle}$ , are 11.73° and 13.34° (see Table S1 of supporting information). Insets: (top right) qualitative comparison between an experiment with a flared nozzle to the 22 July 1980 eruption of Mt. St. Helens (photograph by J. Nieland), (lower left) comparison between an experiment with a narrow straight nozzle and the 21–28 May 2011 Gímsvötn eruption (photograph by S. Linnét). Both comparisons are based on the scale of fingers and layering in the neutral cloud. The arrow labeled “Erosion and Slumping” indicates the evolution of the entrainment coefficient during an eruption as the nozzle evolves from a cylindrical to flared shape. Error bars show measurement uncertainty.

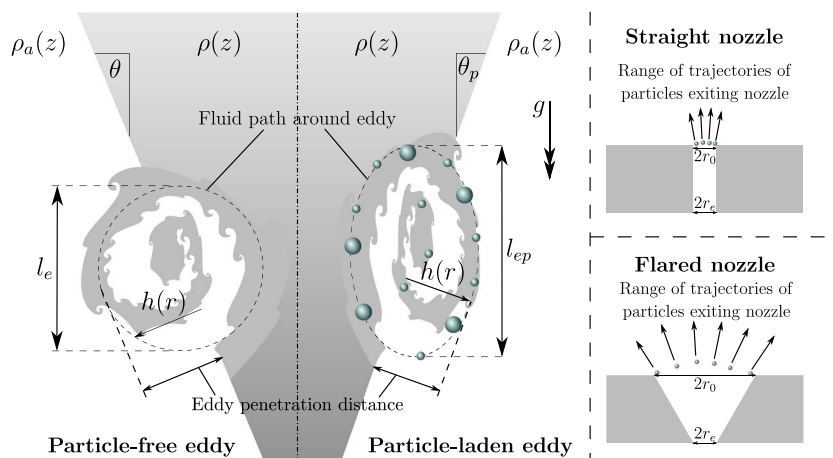


**Figure 3.** (left) Schematic illustrating the ability of a particle-free versus particle-laden eddies to overturn a density interface. In the particle-laden case, vertical stretching of the vortex (characterised by  $l_e$  and  $l_{ep}$ ) leads to a lower capacity for interface overturning, as indicated by the reduced penetration distance,  $h(r)$ . (right) Schematic illustrating the trajectories of particles issuing from flared and straight nozzles. The range of possible trajectories is greater for a flared nozzle than a straight nozzle. The lower diameter of both nozzles,  $r_e$ , is identical.

and angular momentum of these eddies. Whereas  $St \sim 0.1-1$  particles contribute mass and augment the angular momentum of entraining eddies, the nozzle geometry has a crucial effect on the shape of these overturning motions (Figure 3 (right)): cylindrical nozzles restrict particle trajectories to a greater extent than flared nozzles, leading, in turn, to vertically stretched eddies and a smaller average penetration distance  $h$ . Qualitatively, this picture implies that for particle-rich jets erupted from a cylindrical nozzle, less kinetic energy (K.E.) is extracted from the jet velocity field to do the work of mechanical entrainment and mixing against the stabilising environmental stratification. Quantitatively,  $\lambda = 1/\beta = Ri_0/Ri$ , is a measure of the efficiency with which K.E. input at the source is used in mixing. Our results show that  $\lambda_f$  for flared vents is a factor of 25 larger than values for cylindrical vents  $\lambda_c$  and a factor of 20 larger than that for particle free flows  $\lambda$ . The additional lateral momentum flux imparted (indicated by  $\lambda$ ) to the flows as a result of the flared geometry enhances entrainment efficiency and leads to  $\alpha_{e,c} < \alpha_e < \alpha_{e,f}$ , which is consistent with the linear relationship between  $\alpha_e$  and local  $Ri$  proposed by Kaminski *et al.* [2005]. The shaping effect on the momentum flux of cylindrical versus flared nozzles may also play out in the fluid phase, as suggested by fact that the data points for a particle-free flows in narrow and flared nozzles are separated.

Volcanic vents can erode from cylindrical to flared geometries during explosive eruptions. Our results show that this evolution will have a remarkable effect on entrainment (cf. the erosion and slumping arrow in Figure 2) and thus on the structure and height of the volcanic jet and resulting umbrella cloud. In particular, the scale height, given by (1) depends strongly on  $\alpha_e$  and more weakly on  $f_0$ . For example, if during an eruption the vent goes from being straight to flared (i.e.,  $\alpha_e = 0.094 \rightarrow 0.159$  as per our experiments), then the new scale height ( $H_{new}$ ) increases by a factor of  $H_{new}/H_0 = (\alpha_e/\alpha_{e,new})^{1/2}(g'_{new}q_{new}/(g'_0q_0))^{1/4}$ . If the eruption rate and eruptive products remain the same (i.e.,  $q_0 = q_{new}$  and  $g'_0 = g'_{new}$ ), then  $H_{new} = 0.76H_0$ , i.e., the jet height drops by 25%. Such a large reduction in the plume height through this process will cause a monotonic vent ward shift in where the largest pumice clasts and lithic blocks fall to the ground, which should be expressed in the architecture of the deposit. We explore this prediction in detail in a forthcoming paper.

The improved entrainment efficiency that comes with a flared vent means that the jet becomes relatively more buoyant and will overshoot the LNB less. Eruptions with a large overshoot heights form periodically layered umbrella clouds, whereas clouds formed from eruptions with lower overshoots are characterised by lobate fingers or mammata [Carazzo and Jellinek, 2012, 2013, Figure 1, for example]. The two snapshots of volcanic eruptions shown as insets to Figure 2 are possible examples of these two end-members in jet dynamics: in the case of Mt. St. Helens, there is very little overshoot and a lot of large-scale fingers whereas the Grímsvötn eruption has a much larger overshoot region and fine fingering. Sedimentation from these distinctly textured clouds leads to deposits with a fingerprint of the layering regime of the cloud, and hence a link to the state of the vent geometry: sedimentation from clouds with lobate fingers produces stratified

and azimuthally or laterally discontinuous deposits whereas sedimentation from layered clouds produces a uniformly thick layer of fine ash. Our results predict that, as the transition from one vent geometry to another is not only possible but likely, this transition would be recorded in both a decreased overshoot height and the deposit architecture.

## 6. Concluding Remarks

In conventional models for volcanic jets, neither particle inertia nor vent geometry influence the dynamics of entrainment, which is at the heart of predictions for the plume rise height and jet stability. Here we show that entrainment is a sensitive function of vent geometry through its effect on the trajectories of inertial particles. Evolving from a narrow, cylindrical vent to a broad, tapering vent is a natural consequence of mechanical erosion, fracture, and slumping during real eruptions. Such processes will give rise to a decrease in overshoot height of the jet, leading to a change in the shape and dynamics of ash clouds and hence to the structure of air fall deposits from these clouds. Therefore, such deposits may be used as an analytical tool when it comes to classifying historical and prehistoric eruption deposits and determining the source conditions of an eruption.

### Acknowledgments

The authors thank J. Gilchrist for his help in performing the experiments, J. Unger for technical support and construction of the experimental device, and two anonymous reviewers for their constructive comments that improved our manuscript. This work was supported by the Canadian Foundation for Innovation and by NSERC.

The Editor thanks two anonymous reviewers for their assistance evaluating this paper.

### References

- Burgisser, A., G. Bergantz, and R. Breidenthal (2005), Addressing complexity in laboratory experiments: The scaling of dilute multiphase flows in magmatic systems, *J. Volcanol. Geotherm. Res.*, *141*(3–4), 245–265, doi:10.1016/j.jvolgeores.2004.11.001.
- Carazzo, G., and A. M. Jellinek (2012), A new view of the dynamics, stability and longevity of volcanic clouds, *Earth Planet. Sci. Lett.*, *325*, 39–51, doi:10.1016/j.epsl.2012.01.025.
- Carazzo, G., and A. M. Jellinek (2013), Particle sedimentation and diffusive convection in volcanic ash-clouds, *J. Geophys. Res. Solid Earth*, *118*, 1420–1437, doi:10.1002/jgrb.50155.
- Carazzo, G., E. Kaminski, and S. Tait (2006), The route to self-similarity in turbulent jets and plumes, *J. Fluid Mech.*, *547*, 137–148, doi:10.1017/S002211200500683X.
- Carazzo, G., E. Kaminski, and S. Tait (2008), On the rise of turbulent plumes: Quantitative effects of variable entrainment for submarine hydrothermal vents, terrestrial and extra terrestrial explosive volcanism, *J. Geophys. Res.*, *113*, B09201, doi:10.1029/2007JB005458.
- Carey, S., H. Sigurdsson, and R. Sparks (1988), Experimental studies of particle-laden plumes, *J. Geophys. Res.*, *93*(B12), 15,314–15,328, doi:10.1029/JB093iB12p15314.
- Crowe, C., J. Schwarzkopf, M. Sommerfeld, and Y. Tsuji (1997), *Multiphase Flows With Droplets and Particles*, Taylor and Francis, Boca Raton, Fla.
- Dufek, J., and G. W. Bergantz (2007), Suspended load and bed-load transport of particle-laden gravity currents: The role of particle-bed interaction, *Theor. Comput. Fluid Dyn.*, *21*(2), 119–145, doi:10.1007/s00162-007-0041-6.
- Elghobashi, S. (1994), On predicting particle-laden turbulent flows, *Appl. Sci. Res.*, *52*(4), 309–329, doi:10.1007/BF00936835.
- Fan, L.-N. (1967), Turbulent buoyant jets into stratified or flowing ambient fluids, *Tech. Rep. KH-R-15*, California Institute of Technology, Pasadena, Calif.
- Fischer, H., E. List, R. Koh, J. Imberger, and N. Brooks (1979), *Mixing in Inland and Coastal Waters*, Academic Press, New York.
- Kaminski, E., S. Tait, and G. Carazzo (2005), Turbulent entrainment in jets with arbitrary buoyancy, *J. Fluid Mech.*, *526*, 361–376.
- Linden, P. (1973), Interaction of a vortex ring with a sharp density interface - A model for turbulent entrainment, *J. Fluid Mech.*, *60*(3), 467–480, doi:10.1017/S0022112073000303.
- Linden, P. F. (1979), Mixing in stratified fluids, *Geophys. Astrophys. Fluid Dyn.*, *13*(1), 3–23, doi:10.1080/03091927908243758.
- Linden, P. F. (2002), Convection in the environment, in *Perspectives in Fluid Mechanics*, edited by G. K. Batchelor, H. K. Moffatt, and M. G. Worster, chap. 3, pp. 287–343, Cambridge Univ. Press, New York.
- Morton, B. R., G. Taylor, and J. S. Turner (1956), Turbulent gravitational convection from maintained and instantaneous sources, *Proc. R. Soc. London, Ser. A*, *234*(1196), 1–23, doi:10.1098/rspa.1956.0011.
- Papanicolaou, P., and E. List (1988), Investigations of round vertical turbulent buoyant jets, *J. Fluid Mech.*, *195*, 341–391, doi:10.1017/S0022112088002447.
- Raju, N., and E. Meiburg (1997), Dynamics of small, spherical particles in vortical and stagnation point flow fields, *Phys. Fluids*, *9*(2), 299–314, doi:10.1063/1.869150.
- Veitch, G., and A. Woods (2002), Particle recycling in volcanic plumes, *Bull. Volcanol.*, *64*(1), 31–39, doi:10.1007/s00445-001-0180-3.
- Wang, H., and A. Law (2002), Second-order integral model for a round turbulent buoyant jet, *J. Fluid Mech.*, *459*, 397–428, doi:10.1017/S0022112002008157.
- Wilson, L., R. S. J. Sparks, and G. P. L. Walker (1980), Explosive volcanic eruptions - IV: The control of magma properties and conduit geometry on eruption column behaviour, *Geophys. J. R. Astron. Soc.*, *63*(1), 117–148, doi:10.1111/j.1365-246X.1980.tb02613.x.
- Woods, A. (1995), The dynamics of explosive volcanic eruptions, *Rev. Geophys.*, *33*(4), 495–530, doi:10.1029/95RG02096.
- Woods, A., and S. Bower (1995), The decompression of volcanic jets in a crater during explosive volcanic eruptions, *Earth Planet. Sci. Lett.*, *131*(3–4), 189–205, doi:10.1016/0012-821X(95)00012-2.
- Woods, A., and C. Caulfield (1992), A laboratory study of explosive volcanic eruptions, *J. Geophys. Res.*, *97*(B5), 6699–6712, doi:10.1029/92JB00176.
- Woods, A. W. (2010), Turbulent plumes in nature, *Annu. Rev. Fluid Mech.*, *42*, 391–412, doi:10.1146/annurev-fluid-121108-145430.